AD-A096 754 BROWN UNIV PROVIDENCE RI DEPT OF CHEMISTRY F/G 7/2
PREPARATION AND PROPERTIES OF THE SYSTEM FE SUB 1-X CR SUB X NB--ETC(U)
MAR 81 B KHAZAI, R KERSHAW, K DWIGHT, A WOLD N00014-77-C-0387
UNCLASSIFIED TR-15 NL

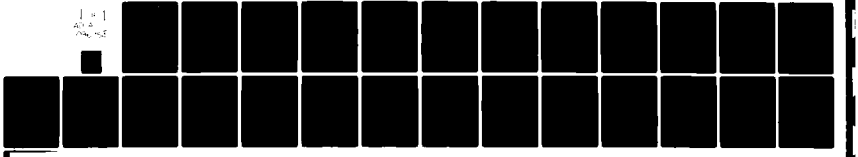

END
DATE FILMED
4 81
DTIC

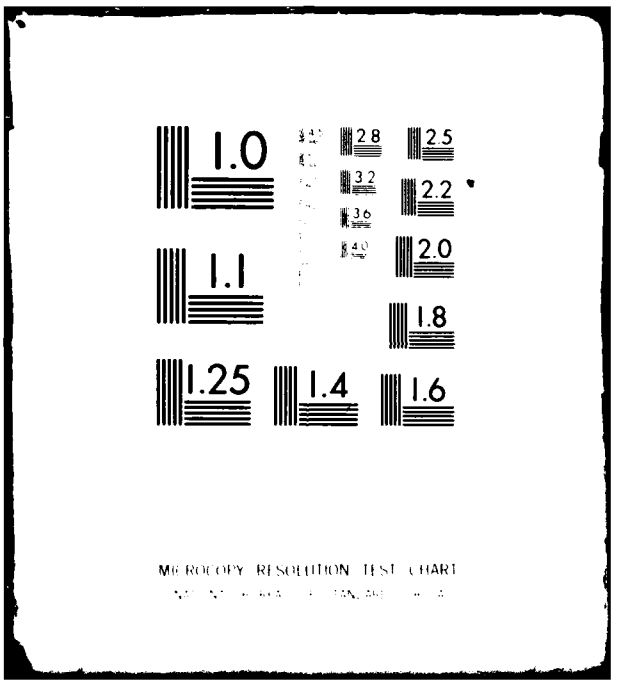
1.0
1.1
1.25
1.4
1.6
1.8
2.0
2.2
2.5
2.8
3.2
3.6
4.0
MICROCOPY RESOLUTION TEST CHART

LEVEL II

(12)

SECURITY CLASSIFICATION OF THIS PAGE (When Data Entered)

REPORT DOCUMENTATION PAGE	READ INSTRUCTIONS BEFORE COMPLETING FORM
1. REPORT NUMBER: 15	2. GOVT ACCESSION NO.: AD-A096754	3. RECIPIENT'S CATALOG NUMBER
4. TITLE (and Subtitle): Preparation and Properties of the System $Fe_{1-x}Cr_xNbO_4$	5. TYPE OF REPORT & PERIOD COVERED: Technical
	6. PERFORMING ORG. REPORT NUMBER: 15
7. AUTHOR(s): B. Khazai, R. Kershaw, K. Dwight and A. Wold	8. CONTRACT OR GRANT NUMBER(s): N00014-77-C-0387
9. PERFORMING ORGANIZATION NAME AND ADDRESS: Professor Aaron Wold, Brown University, Department of Chemistry, Providence, Rhode Island 02912	10. PROGRAM ELEMENT, PROJECT, TASK AREA & WORK UNIT NUMBERS: NR-359-653
11. CONTROLLING OFFICE NAME AND ADDRESS: Dr. David Nelson, Code 472, Office of Naval Research, Arlington, Virginia 22217	12. REPORT DATE: March 20, 1981
	13. NUMBER OF PAGES: 26
14. MONITORING AGENCY NAME & ADDRESS (if different from Controlling Office)	15. SECURITY CLASS. (of this report)
	15a. DECLASSIFICATION DOWNGRADING SCHEDULE

16. DISTRIBUTION STATEMENT (of this Report)

Approved for Public Release; Distribution Unlimited

17. DISTRIBUTION STATEMENT (of the abstract entered in Block 20, if different from Report)

18. SUPPLEMENTARY NOTES

Submitted to the Journal of Solid State Chemistry

19. KEY WORDS (Continue on reverse side if necessary and identify by block number)

Chromium-substituted Iron Niobates
Increased Response at Longer Wavelengths
Lowering of Optical Band Gap

20. ABSTRACT (Continue on reverse side if necessary and identify by block number)

Members of the system $Fe_{1-x}Cr_xNbO_4$ were prepared and their magnetic and electronic properties investigated. It was shown that chromium substitution favored the formation of the rutile structure, which resulted in a decrease in the electrical conductivity because of randomization of the transition metal ions in the structure. The replacement of a few percent of Fe^{3+} with Cr^{3+} caused a significant lowering of the lowest optical band gap, whereas the higher energy transitions remained essentially unchanged. This resulted in increased response to the longer wavelengths of the solar spectrum.

DD FORM 1 JAN 73 1473 EDITION OF 1 NOV 65 IS OBSOLETE S/N 0102-014-6601

SECURITY CLASSIFICATION OF THIS PAGE (When Data Entered)

(14) TK-15

OFFICE OF NAVAL RESEARCH

(15) Contract N00014-77-C-0387

Task No. NR-359-653

(9) TECHNICAL REPORT NO. 15

(6) Preparation and Properties of the System $Fe_{1-x}Cr_xNbO_4$

Fe sub 1-x Cr sub x NbO4

by

(10) B. Khazai, R. Kershaw, K. Dwight and A. Wold

(11) 30 Mar 81

Prepared for Publication

(12) 26

in the

Journal of Solid State Chemistry

Brown University

Department of Chemistry

Providence, Rhode Island

March 30, 1981

INTRODUCTION

The binary oxide of niobium, Nb_2O_5, has been reported to have an optical band gap of 3.4 eV (1). This would suggest that such a material, when used as an n-type photoanode for the photoassisted decomposition of water, would be limited in its absorptivity to the ultra-violet region of the spectrum (λ<400nm). In $Sr_2Nb_2O_7$, where NbO_6 octahedra are the photoactive centers, the material shows a band gap of 3.86 eV without any significant absorption of the visible radiation (2). However, it has been shown that the association of Fe_2O_3, band gap 2.2 eV (3), with Nb_2O_5 in $FeNbO_4$ results in enhancement of quantum efficiency, as well as extension of absorption to longer wavelengths (4). It has also been reported recently (5) that Cr^{3+} doped TiO_2 shows photocurrents resulting from low-energy electronic excitations, which would indicate a lowering of the optical band gap. Such an observation, along with the low band gap of Cr_2O_3, 1.4 eV (6), would suggest the use of chromium as a possible dopant in order to produce more efficient photoanodes.

It was indicated in an earlier publication (4) that $FeNbO_4$ can form a solid solution with $FeNb_2O_6$, which would give rise to a conducting oxide. Such a compound, where the different valencies of the transition metal ion are located at identical lattice sites, should also show interesting magnetic properties resulting from interaction of 3d electrons. In this study, the effect of the substitution of chromium for iron on the electronic and magnetic properties of $FeNbO_4$ will be reported.

EXPERIMENTAL

Synthesis

All materials were prepared from the solid state reaction between Fe_2O_3 (Johnson-Matthey, spec pure), Nb_2O_5 (Kawecki Berylco Industries, spectroscopic grade), and Cr_2O_3 which was obtained by the careful thermal decomposition of ammonium dichromate (Allied Chemical Co.). Iron niobate, as well as the chromium substituted samples, was prepared by placing a finely ground mixture of appropriate amounts of the starting materials in a platinum crucible and heating in air at 1150 °C for 48 hours. Each sample was x-rayed and then reheated. After a third heating, the product was cooled to room temperature in the furnace and re-examined by x-ray analysis. This was done in order to confirm the formation of a single phase. A Philips Norelco diffractometer, with CuKα radiation (1.5405Å) at a scan rate of 0.25° 2θ/min, was used.

Discs were formed by pressing aliquots of approximately 150mg at 90,000 p.s.i.; five drops of Carbowax were added to the powder before pressing, in order to facilitate the formation of a well-sintered disc. The pressed discs were placed on a bed of powder having the same composition in an alumina crucible. The discs were heated in a hollow globar furnace at a rate of 85° per hour to 1250 °C and maintained at that temperature for 24 hours. At the end of the sintering process, the discs were cooled at the same rate.

X-ray diffraction patterns of the sintered discs showed, at the limit of detection, the presence of the strongest line of α-Fe_2O_3, which is consistent with the formation of a solid solution of $FeNb_2O_6$ in $FeNbO_4$ under the

sintering conditions. Essentially identical resistivities were measured before and after abrading these discs to one-half their original thickness, establishing their homogeneity.

Magnetic Measurements

Magnetic susceptibilities were measured using a Faraday balance (7) over the range from liquid nitrogen to room temperature at a field strength of 10.4 kOe. Honda-Owen (field dependency) plots were also made to determine the presence or absence of ferromagnetic impurities. The data were then corrected for core diamagnetism (8).

Electrical Measurements

The resistivities of the samples were measured using the Van der Pauw technique (9). Contacts were made by the ultrasonic soldering of indium directly onto the samples, and their ohmic behavior was established by measuring their current-voltage characteristics.

Electrode Preparation

Photoanodes were prepared by evaporating thin films of gold on the backs of the discs to provide good electrical contact. The gold face of each disc was attached to the electrode by means of indium solder. Miccrostop (Michigan Chrome Chemical Corp.) was applied to the gold face and the electrode wire for insulation. The photoelectrolysis measurements were carried out with a 150 watt xenon lamp, a monochromator (Oriel Model 7240), a glass cell with a quartz window, and a current amplifier as described previously (10).

The electrolyte, 0.2M sodium acetate (pH = 7.8), was purged of dissolved oxygen by continuous bubbling of 85% argon-15% hydrogen gas.

Structure

$FeNbO_4$ has been reported to crystallize with the monoclinic wolframite structure (space group P2/C) below 1085 °C. Roth (11) and Laves (12) have shown that between 1085 °C and 1380 °C, a transition to the orthorhombic α-PbO_2 structure (space group Pbcn) occurs, followed by a further transformation to the tetragonal rutile structure (space group $P4_2/mnm$) above 1380°C.

In the rutile form of $FeNbO_4$, shown in figure 1(a), it can be seen that the octahedra share edges in such a way that straight chains are formed along the c direction (perpendicular to the plane of the paper). As shown in figure 1(b), there is a random distribution of Fe and Nb atoms in one half of the available octahedral sites. On the other hand, when $FeNbO_4$ crystallizes with the α-PbO_2 structure, the MO_6 units are joined in such a way as to form zig-zag chains of octahedra along the c direction (figure 2). As with the rutile structure, only one half of the octahedral sites are occupied, and random distribution of Fe and Nb atoms in the zig-zag chains prevails. The wolframite polymorph (figure 3) is an ordered variant of the α-PbO_2 structure in which the Fe and Nb atoms are distributed in such a fashion that every occupied chain contains either only Fe or only Nb atoms. The transformation of wolframite to α-PbO_2, which occurs at elevated temperatures, is therefore considered to be the result of randomization of Fe and Nb atoms within the structural array.

Thus, for $FeNbO_4$, the rutile and α-PbO_2 are related to the nature of the chains formed, i.e., straight or zig-zag. In both polymorphs, the Fe and Nb atoms are arranged in a random fashion. Ordering of the atoms has been observed in the zig-zag chains, and such ordering gives rise to the formation of the wolframite structure.

RESULTS

The system $Fe_{1-x}Cr_xNbO_4$ forms a solid solution crystallizing with the wolframite structure over a composition range of $0<x<0.1$. In the region $0.1<x<0.4$, a mixture of the wolframite $FeNbO_4$ and rutile $CrNbO_4$ phases was obtained. Between $0.4\leq x\leq 1$, the products can be indexed on the basis of the rutile $CrNbO_4$ structure. The precision lattice parameters are listed in Table I. The changes in the cell parameters may be attributed to the difference in the ionic radii of Fe^{3+}(0.65Å) and Cr^{3+}(0.615Å). Table II indicates the change in the electrical resistivities in going from the wolframite compositions to those of the rutile. The electrical resistivity is enhanced greatly as the structure is transformed from wolframite to rutile. The resistivity varies from 53 ohm-cm for x=0.1 (wolframite) to an insulator for x=0.4 (rutile). Such a difference can be explained in terms of the ordering of iron and niobium chains in the wolframite structure. As indicated previously (4), $FeNbO_4$ can form a solid solution with $FeNb_2O_6$. Cation ordering of the zig-zag chains prevents the Nb^{5+} ions from blocking the conduction paths which result from the co-existence of Fe^{2+} and Fe^{3+} ions in the alternate chains (figure 3). This gives rise to the observed increase in conductivity. For products which crystallize with the straight-chain rutile structure, there is a lack of ordering of the FeO_6 and NbO_6 octahedra, and hence, low electrical conductivity is observed.

The magnetic data for the system $Fe_{1-x}Cr_xNbO_4$ is summarized in Table II. All compositions show Curie-Weiss behavior with effective molar Curie constants, C_M, corresponding to those expected from spin-only moment

considerations involving primarily Fe^{3+} , Cr^{3+} , and Nb^{5+} . A high spin state for both Fe^{3+} and Cr^{3+} ($\mu_{eff}Nb^{5+}=0$) is assumed. From Table II, it can be seen that the value of the paramagnetic Curie temperature, θ, is negative and decreases in magnitude with increasing chromium substitution. The decrease in the θ values given in Table II is attributed to a decrease in the strength of the antiferromagnetic interactions, caused by the substitution of d^3 chromium for d^5 iron.

The photoresponse observed for the chromium-doped $FeNbO_4$ is represented in figure 4, where the photocurrents obtained in the "white" light are plotted against the anode potential measured with respect to a standard calomel electrode (SCE). The photoresponse curve for $FeNbO_4$ (4) is included for comparison. The general shapes of the two curves are quite similar. Although the onset of photocurrent is not sufficiently abrupt for an exact comparison of the flat-band potentials, there does not appear to be a significant shift, and as can be seen, the flat-band potential seems to lie between 0.1 and 0.4V vs SCE for both compounds.

The quantum efficiency η (in electrons/photon) of $Fe_{.9}Cr_{.1}NbO_4$, as measured at an anode potential of 0.8V vs SCE, is plotted in figure 5. Results for $FeNbO_4$ are again included for the purpose of comparison. Although the shapes of the spectral response curves remain similar, the photoresponse of the chromium-doped sample extends to longer wavelengths and possesses higher efficiency in the visible part of the spectrum. This increase in efficiency is sufficient to nearly double the total photoresponse to AM1 (air mass 1) solar irradiation, as can be seen from figure 6. Such an extension to longer

wavelengths was also observed for the chromium-substituted systems $Ti_{1-x}Cr_xO_2$ and $BaTi_{1-x}Cr_xO_3$ (5,13,14). Unfortunately, further improvement of the photoresponse at higher wavelengths for chromium-substituted $FeNbO_4$ could not be achieved because of the high resistivity of the rutile phases.

Analysis of the spectral response data can yield values for the various energy transitions (15). Accordingly, the quantity $(\eta h\nu)^{0.5}$ is plotted as a function of the photon energy in figure 7. This analysis yields a lowest-energy optical band gap of 1.90(5) eV. As previously reported, $FeNbO_4$ shows a lowest-energy transition of 2.08 eV. Consequently, there appears to be a significant lowering of the band gap on substitution of small amounts of chromium into $FeNbO_4$. This is in good agreement with the reported decrease in the optical band gap of α-Fe_2O_3 for a 10 mole percent substitution of chromium (16). In addition, from the data presented in figure 7, several additional band transitions at higher energies can be estimated. These are indicated by sudden increases in the slope, such as occur at 2.7(1), 3.27(3) and 4.41(2)eV. The latter three energy gaps agree quite closely with the values of 2.68(2), 3.24(4), and 4.38(2) eV reported for pure $FeNbO_4$. Such an agreement suggests that the individual characteristics of FeO_6 and NbO_6 centers of $FeNbO_4$ are not altered. The lowering of the optical band gap can, therefore, be attributed to the formation of Cr^{3+} $(3d^3)$ energy levels within the optical band gap of $FeNbO_4$. However, as suggested by Goodenough (14) and Campet (5), some surface delocalization of $Cr^{3+}(3d^3)$ states are probably required to make the observed contributions to photoactivity possible.

TABLE I

Precision Lattice Constants for the System $Fe_{1-x}Cr_xNbO_4$

	a(Å)	b(Å)	c(Å)	β(deg.)
$FeNbO_4$	4.997(2)	5.619(2)	4.651(2)	90
$Fe_{.9}Cr_{.1}NbO_4$	4.996(2)	5.611(2)	4.642(2)	89.79
$Fe_{.6}Cr_{.4}NbO_4$	4.670(2)	-	3.030(2)	-
$CrNbO_4$	4.645(2)	-	3.012(2)	-

TABLE II

Magnetic and Electrical Data on the System $Fe_{1-x}Cr_xNbO_4$

	Structure[(a)]	C_M expt'l	C_M theo.	θ	ρ (ohms)
$FeNbO_4$	W	4.18	4.35	-79.8	40(1)
$Fe_{.9}Cr_{.1}NbO_4$	W	3.80	3.94(b)	-52.6	53(1)
$CrNbO_4$	R	1.87	1.87	-33.9	insul.

(a) W = Wolframite, R = rutile

(b) Corrected for $C_M(Fe^{3+}) = 4.18$

ACKNOWLEDGEMENTS

The Office of Naval Research, Arlington, Virginia, supported the work of Bijan Khazai and Kirby Dwight. In addition, the authors would like to acknowledge the support of the Materials Research Laboratory Program at Brown University.

REFERENCES

1. P. Clechet, J. Martin, R. Oliver and C. Vallouy, C. R. Acad. Sci. Paris, Ser. C282, 887 (1976).

2. J. Hormadaly, S. N. Subbarao, R. Kershaw, K. Dwight and A. Wold, J. Solid State Chem. 33, 27 (1980).

3. W. H. Strehlow and E. L. Cook, J. Phys. Chem. Ref. Data, 2, 163 (1973).

4. J. Koenitzer, B. Khazai, J. Hormadaly, R. Kershaw, K. Dwight and A. Wold, J. Solid State Chem. 35, 128 (1980).

5. G. Campet, J. Verniolle, J. P. Doumec and J. Claverie, Mat. Res. Bull. 15, 1135 (1980).

6. H. P. Maruska and A. Ghosh, Solar Energy 20, 443 (1978).

7. B. Morris and A. Wold, Rev. Sci. Inst. 39, 1937 (1968).

8. P. W. Selwood, "Magnetochemistry " 2nd ed., Interscience Pub. Co.,(1956).

9. L. J. Van der Pauw, Philips Res. Rep. 13, 1 (1968).

10. S. N. Subbarao, Y. H. Yun, R. Kershaw, K. Dwight and A. Wold, Inorg. Chem. 18, 488 (1979).

11. R. S. Roth and J. Waring, Amer. Mineral. 49, 243 (1964).

12. Von F. Laves, G. Bayer and A. Panagos, Schweiz. Mineral. Petrog. Mitt. 43, 217 (1963).

13. A. Monnier and J. Augustinski, J. Electrochem. Soc. 127, No7, 1576 (1980).

14. G. Campet, M. P. Dare-Edwards, A. Hammett and J. B. Goodenough, Nouveau Journal de Chemie, 4,No. 819, 501 (1980).

15. F. P. Koffyberg, K. Dwight and A. Wold, Solid State Commun. 30, 433 (1979).

16. P. Merchant, R. Collins, R. Kershaw, K. Dwight and A. Wold, J. Solid State Chem. 27, 307 (1979).

FIGURE CAPTIONS

Figure 1. The structure of rutile, MO_2: (a) packing of MO_6 octahedra; (b) closest-packed arrangement of oxygen around M atoms.

Figure 2. The structure of α-PbO_2: (a) packing of MO_6 octahedra; (b) closest-packed arrangement of oxygen around M atoms.

Figure 3. Structure of Wolframite $FeNbO_4$: (a) packing of MO_6 octahedra; (b) closest-packed layer of oxygen around Fe and Nb Atoms.

Figure 4. Variation of photocurrent with anode potential under "white" xenon arc irradiation of 1.0 w/cm^2 in 0.2 M sodium acetate adjusted to pH=7.8

Figure 5. Spectral variation of the quantum efficiency obtained at an anode potential of 0.8 volts vs SCE in 0.2 M sodium acetate adjusted to pH=7.8

Figure 6. Solar response for air mass 1 (AM1) calculated from the data presented in figure 5.

Figure 7. Indirect band-gap analysis for $Fe_{0.9}Cr_{0.1}NbO_4$, showing transitions at 1.90(5), 2.7(1), 3.27(3) and 4.41(2) eV.

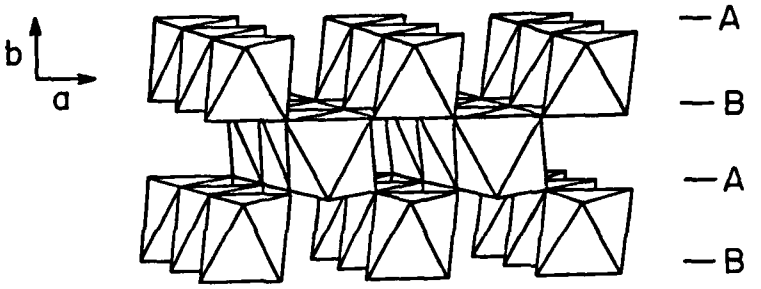

(a)

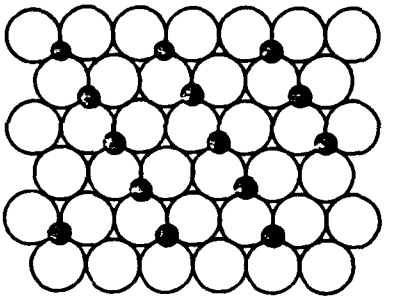

(b)

● Fe/Nb

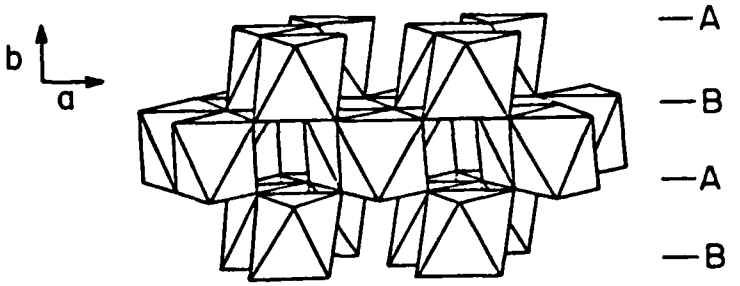

(a)

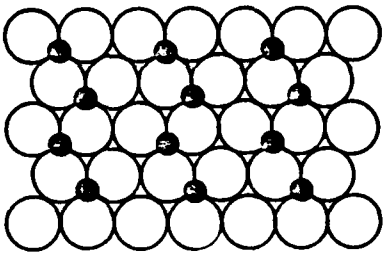

(b)

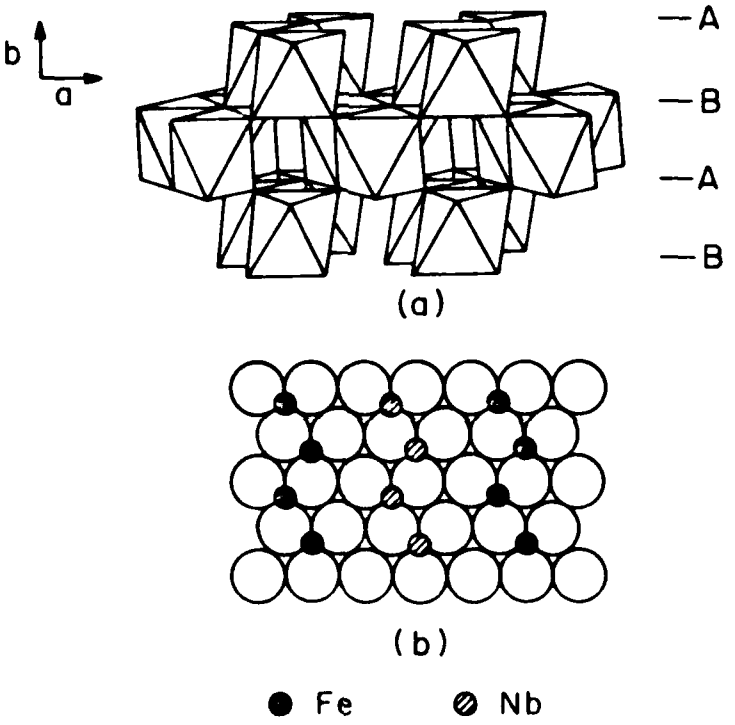
b
a
A
B
A
B
(a)
(b)
Fe
Nb

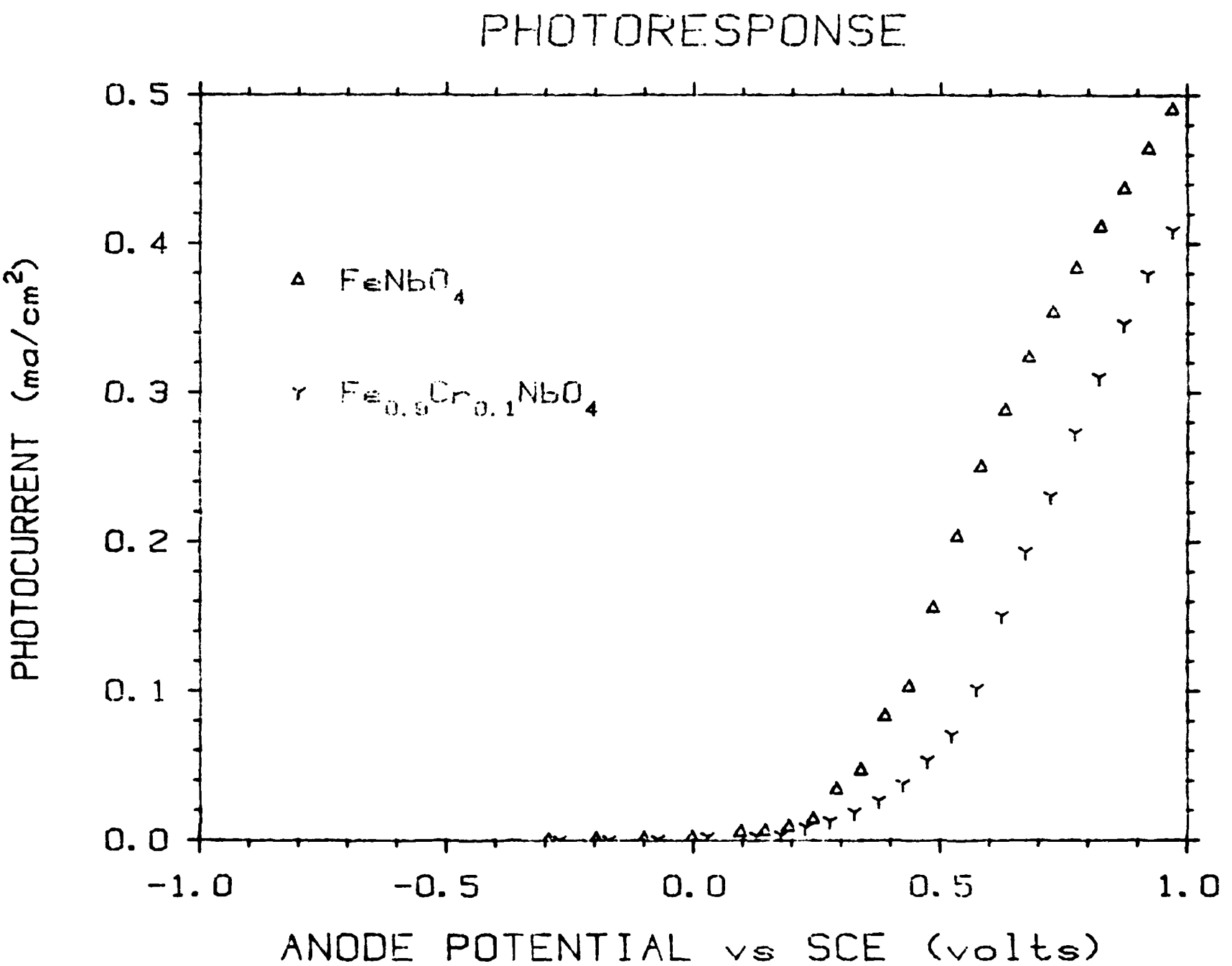
PHOTORESPONSE
PHOTOCURRENT (ma/cm²)
0.5
0.4
0.3
0.2
0.1
0.0
FeNbO4
Fe0.9Cr0.1NbO4
-1.0
-0.5
0.0
0.5
1.0
ANODE POTENTIAL vs SCE (volts)

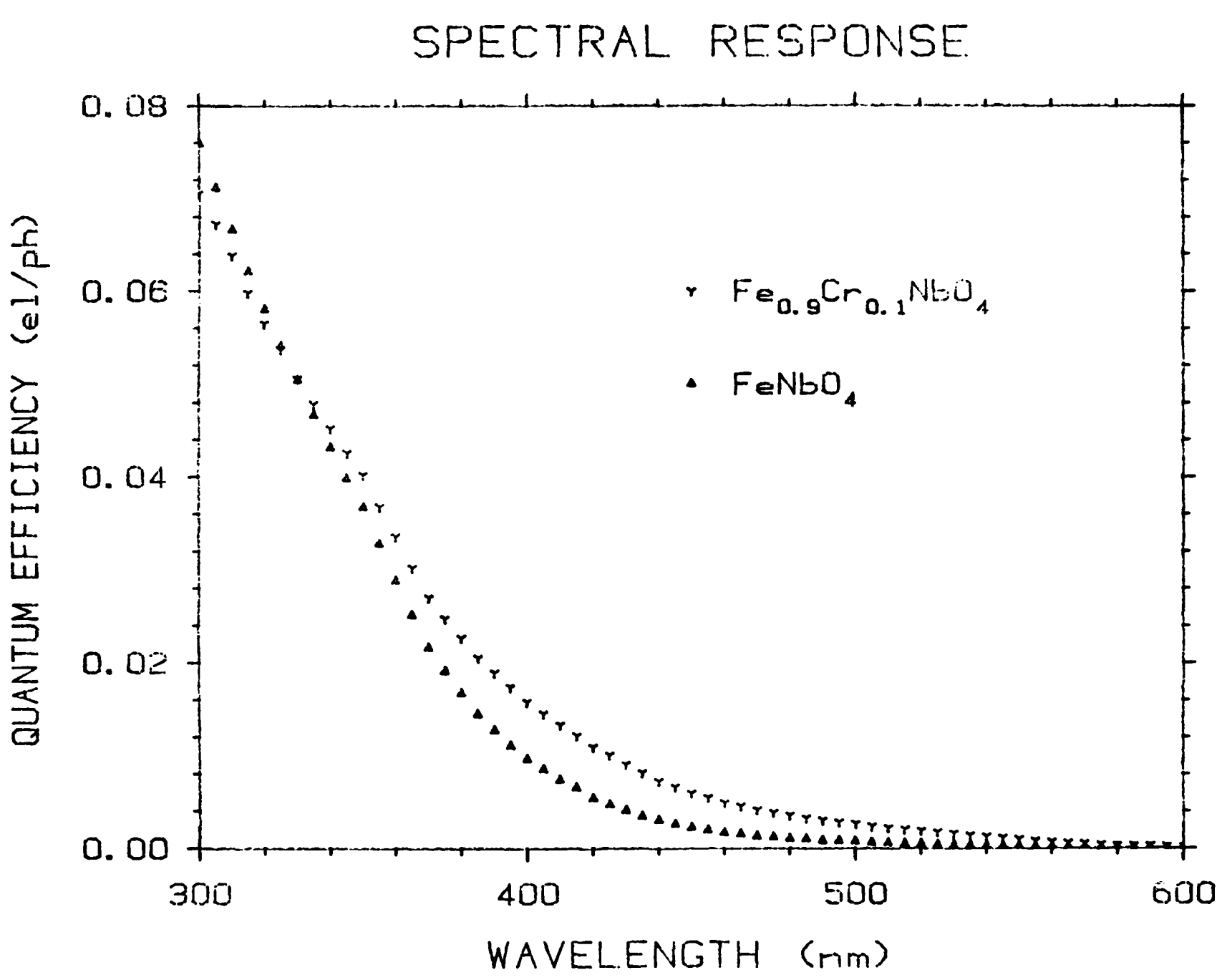
SPECTRAL RESPONSE
0.08
0.06
0.04
0.02
0.00
QUANTUM EFFICIENCY (el/ph)
300
400
500
600
WAVELENGTH (nm)
Fe0.9Cr0.1NbO4
FeNbO4

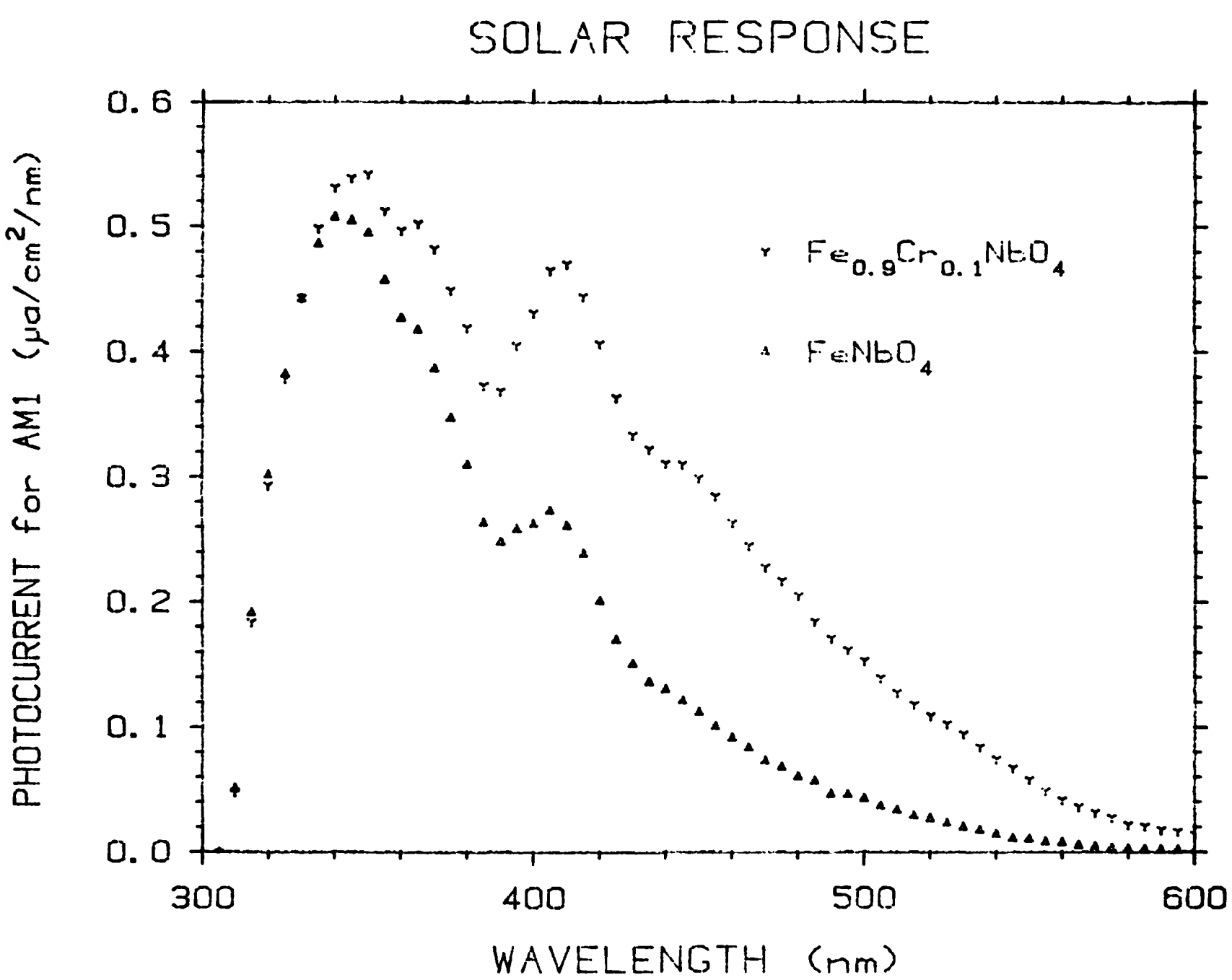
SOLAR RESPONSE
PHOTOCURRENT for AM1 (μa/cm²/nm)
0.6
0.5
0.4
0.3
0.2
0.1
0.0
300
400
500
600
WAVELENGTH (nm)
Fe0.9Cr0.1NbO4
FeNbO4

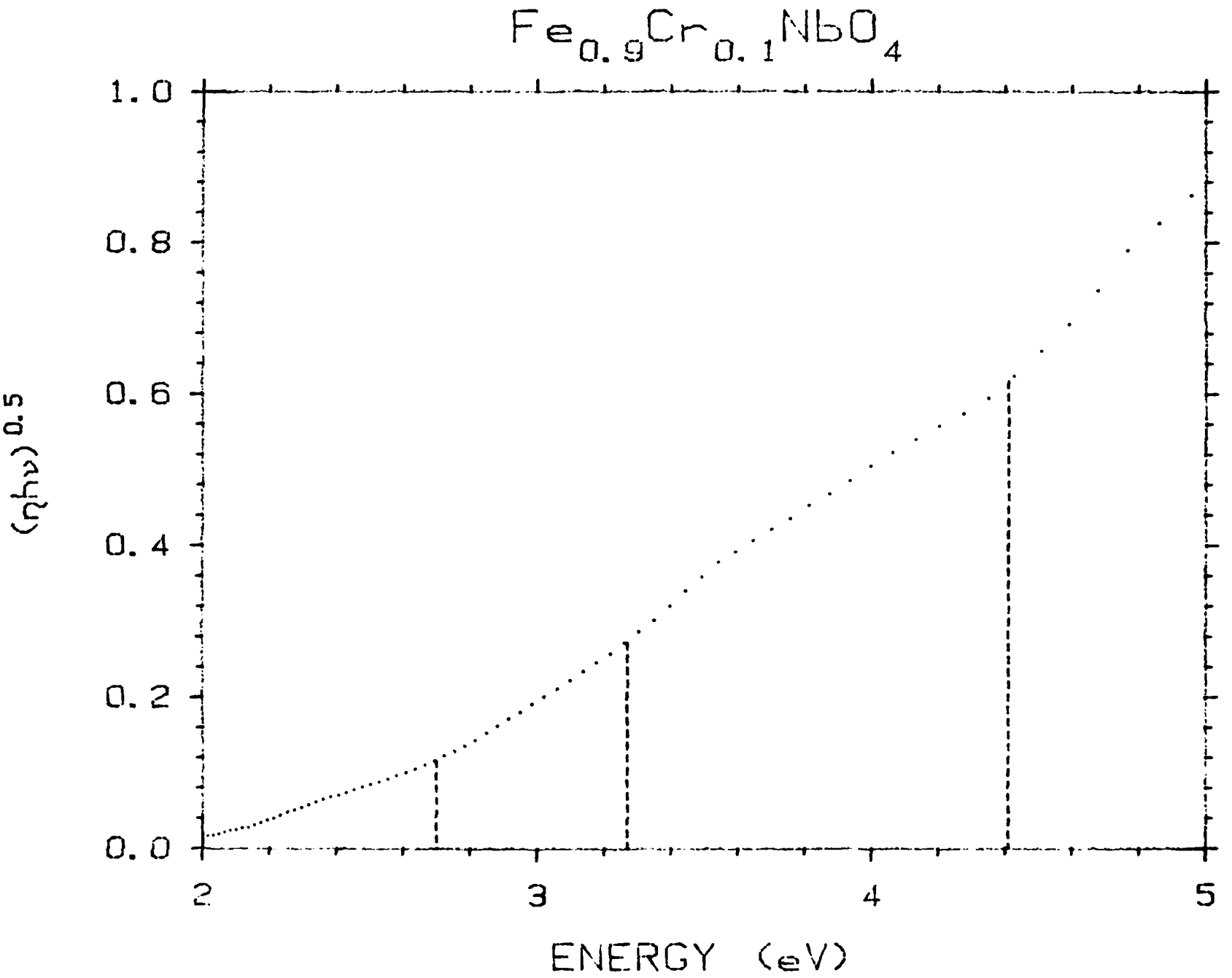
$Fe_{0.9}Cr_{0.1}NbO_4$
1.0
0.8
0.6
0.4
0.2
0.0
$(\eta h\nu)^{0.5}$
2
3
4
5
ENERGY (eV)

TECHNICAL REPORT DISTRIBUTION LIST, GEN

	No. Copies
Office of Naval Research Attn: Code 472 800 North Quincy Street Arlington, Virginia 22217	2
ONR Branch Office Attn: Dr. George Sandoz 536 S. Clark Street Chicago, Illinois 60605	1
ONR Area Office Attn: Scientific Dept. 715 Broadway New York, New York 10003	1
ONR Western Regional Office 1030 East Green Street Pasadena, California 91106	1
ONR Eastern/Central Regional Office Attn: Dr. L. H. Peebles Building 114, Section D 666 Summer Street Boston, Massachusetts 02210	1
Director, Naval Research Laboratory Attn: Code 6100 Washington, D.C. 20390	1
The Assistant Secretary of the Navy (RE&S) Department of the Navy Room 4E736, Pentagon Washington, D.C. 20350	1
Commander, Naval Air Systems Command Attn: Code 310C (H. Rosenwasser) Department of the Navy Washington, D.C. 20360	1
Defense Technical Information Center Building 5, Cameron Station Alexandria, Virginia 22314	12
Dr. Fred Saalfeld Chemistry Division, Code 6100 Naval Research Laboratory Washington, D.C. 20375	1
U.S. Army Research Office Attn: CRD-AA-IP P.O. Box 1211 Research Triangle Park, N.C. 27709	1
Naval Ocean Systems Center Attn: Mr. Joe McCartney San Diego, California 92152	1
Naval Weapons Center Attn: Dr. A. B. Amster, Chemistry Division China Lake, California 93555	1
Naval Civil Engineering Laboratory Attn: Dr. R. W. Drisko Port Hueneme, California 93401	1
Department of Physics & Chemistry Naval Postgraduate School Monterey, California 93940	1
Dr. A. L. Slafkosky Scientific Advisor Commandant of the Marine Corps (Code RD-1) Washington, D.C. 20380	1
Office of Naval Research Attn: Dr. Richard S. Miller 800 N. Quincy Street Arlington, Virginia 22217	1
Naval Ship Research and Development Center Attn: Dr. G. Bosmajian, Applied Chemistry Division Annapolis, Maryland 21401	1
Naval Ocean Systems Center Attn: Dr. S. Yamamoto, Marine Sciences Division San Diego, California 91232	1
Mr. John Boyle Materials Branch Naval Ship Engineering Center Philadelphia, Pennsylvania 19112	1

TECHNICAL REPORT DISTRIBUTION LIST, GEN

	No. Copies
Dr. Rudolph J. Marcus Office of Naval Research Scientific Liaison Group American Embassy APO San Francisco 96503	1
Mr. James Kelley DTNSRDC Code 2803 Annapolis, Maryland 21402	1

TECHNICAL REPORT DISTRIBUTION LIST, 359

	No. Copies
Dr. Paul Delahay Department of Chemistry New York University New York, New York 10003	1
Dr. E. Yeager Department of Chemistry Case Western Reserve University Cleveland, Ohio 41106	1
Dr. D. N. Bennion Department of Chemical Engineering Brigham Young University Provo, Utah 84602	1
Dr. R. A. Marcus Department of Chemistry California Institute of Technology Pasadena, California 91125	1
Dr. J. J. Auborn Bell Laboratories Murray Hill, New Jersey 07974	1
Dr. Adam Heller Bell Laboratories Murray Hill, New Jersey 07974	1
Dr. T. Katan Lockheed Missiles & Space Co, Inc. P.O. Box 504 Sunnyvale, California 94088	1
Dr. Joseph Singer, Code 302-1 NASA-Lewis 21000 Brookpark Road Cleveland, Ohio 44135	1
Dr. B. Brummer EIC Incorporated 55 Chapel Street Newton, Massachusetts 02158	1
Library P. R. Mallory and Company, Inc. Northwest Industrial Park Burlington, Massachusetts 01803	1
Dr. P. J. Hendra Department of Chemistry University of Southhampton Southhampton SO9 5NH United Kingdom	1
Dr. Sam Perone Department of Chemistry Purdue University West Lafayette, Indiana 47907	1
Dr. Royce W. Murray Department of Chemistry University of North Carolina Chapel Hill, North Carolina 27514	1
Naval Ocean Systems Center Attn: Technical Library San Diego, California 92152	1
Dr. C. E. Mueller The Electrochemistry Branch Materials Division, Research & Technology Department Naval Surface Weapons Center White Oak Laboratory Silver Spring, Maryland 20910	1
Dr. G. Goodman Globe-Union Incorporated 5757 North Green Bay Avenue Milwaukee, Wisconsin 53201	1
Dr. J. Boechler Electrochimica Corporation Attention: Technical Library 2485 Charleston Road Mountain View, California 94040	1
Dr. P. P. Schmidt Department of Chemistry Oakland University Rochester, Michigan 48063	1
Dr. H. Richtol Chemistry Department Rensselaer Polytechnic Institute Troy, New York 12181	1

TECHNICAL REPORT DISTRIBUTION LIST, 359

	No. Copies
Dr. A. B. Ellis Chemistry Department University of Wisconsin Madison, Wisconsin 53706	1
Dr. M. Wrighton Chemistry Department Massachusetts Institute of Technology Cambridge, Massachusetts 02139	1
Larry E. Plew Naval Weapons Support Center Code 30736, Building 2906 Crane, Indiana 47522	1
S. Ruby DOE (STOR) 600 E Street Washington, D.C. 20545	1
Dr. Aaron Wold Brown University Department of Chemistry Providence, Rhode Island 02192	1
Dr. R. C. Chudacek McGraw-Edison Company Edison Battery Division Post Office Box 28 Bloomfield, New Jersey 07003	1
Dr. A. J. Bard University of Texas Department of Chemistry Austin, Texas 78712	1
Dr. M. M. Nicholson Electronics Research Center Rockwell International 3370 Miraloma Avenue Anaheim, California	1
Dr. Donald W. Ernst Naval Surface Weapons Center Code R-33 White Oak Laboratory Silver Spring, Maryland 20910	1
Dr. R. P. Van Duyne Department of Chemistry Northwestern University Evanston, Illinois 60201	1
Dr. B. Stanley Pons Department of Chemistry University of Alberta Edmonton, Alberta CANADA T6G 2G2	1
Dr. Michael J. Weaver Department of Chemistry Michigan State University East Lansing, Michigan 48824	1
Dr. R. David Rauh EIC Corporation 55 Chapel Street Newton, Massachusetts 02158	1
Dr. J. David Margerum Research Laboratories Division Hughes Aircraft Company 3011 Malibu Canyon Road Malibu, California 90265	1
Dr. Martin Fleischmann Department of Chemistry University of Southampton Southampton SO9 5NH England	1
Dr. Janet Osteryoung Department of Chemistry State University of New York at Buffalo Buffalo, New York 14214	1
Dr. R. A. Osteryoung Department of Chemistry State University of New York at Buffalo Buffalo, New York 14214	1
Mr. James R. Moden Naval Underwater Systems Center Code 3632 Newport, Rhode Island 02840	1

TECHNICAL REPORT DISTRIBUTION LIST, 359

	No. Copies
Dr. R. Nowak Naval Research Laboratory Code 6130 Washington, D.C. 20375	1
Dr. John F. Houlihan Shenango Valley Campus Pennsylvania State University Sharon, Pennsylvania 16146	1
Dr. M. G. Sceats Department of Chemistry University of Rochester Rochester, New York 14627	1
Dr. D. F. Shriver Department of Chemistry Northwestern University Evanston, Illinois 60201	1
Dr. D. H. Whitmore Department of Materials Science Northwestern University Evanston, Illinois 60201	1
Dr. Alan Bewick Department of Chemistry The University Southampton, S09 5NH England	1
Dr. A. Himy NAVSEA-5433 NC #4 2541 Jefferson Davis Highway Arlington, Virginia 20362	1
Dr. John Kincaid Department of the Navy Stategic Systems Project Office Room 901 Washington, DC 20376	1
M. L. Robertson Manager, Electrochemical Power Sonices Division Naval Weapons Support Center Crane, Indiana 47522	1
Dr. Elton Cairns Energy & Environment Division Lawrence Berkeley Laboratory University of California Berkeley, California 94720	1
Dr. Bernard Spielvogel U.S. Army Research Office P.O. Box 12211 Research Triangle Park, NC 27709	1
Dr. Denton Elliott Air Force Office of Scientific Research Bldg. 104 Bolling AFB Washington, DC 20332	1


DAT
FILM